Journal of Hazardous Materials 181 (2010) 432–439

Contents lists available at ScienceDirect

Journal of Hazardous Materials

journal homepage: www.elsevier.com/locate/jhazmat

Thermal behaviors, nonisothermal decomposition reaction kinetics, thermal safety and burning rates of BTATz-CMDB propellant

Jian-Hua Yi[a], Feng-Qi Zhao[a,*], Bo-Zhou Wang[a], Qian Liu[a], Cheng Zhou[a], Rong-Zu Hu[a], Ying-Hui Ren[b], Si-Yu Xu[a], Kang-Zhen Xu[b], Xiao-Ning Ren[a]

[a] Xi'an Modern Chemistry Research Institute, Xi'an 710065, PR China
[b] School of Chemical Engineering, Northwest University, Xi'an 710069, PR China

ARTICLE INFO

Article history:
Received 3 February 2010
Received in revised form 5 May 2010
Accepted 6 May 2010
Available online 13 May 2010

Keywords:
3,6-Bis(1H-1,2,3,4-tetrazol-5-yl-amino)-1,2,4,5-tetrazine
(BTATz)
Composite modified double base (CMDB) propellant
Nonisothermal kinetics
Thermal safety
Burning rate

ABSTRACT

The composite modified double base (CMDB) propellants (nos. RB0601 and RB0602) containing 3,6-bis (1H-1,2,3,4-tetrazol-5-yl-amino)-1,2,4,5-tetrazine (BTATz) without and with the ballistic modifier were prepared and their thermal behaviors, nonisothermal decomposition reaction kinetics, thermal safety and burning rates were investigated. The results show that there are three mass-loss stages in TG curve and two exothermic peaks in DSC curve for the BTATz-CMDB propellant. The first two mass-loss stages occur in succession and the temperature ranges are near apart, and the decomposition peaks of the two stages overlap each other, inducing only one visible exothermic peak appear in DSC curve during 350–550 K. The reaction mechanisms of the main exothermal decomposition processes of RB0601 and RB0602 are all classified as chemical reaction, the mechanism functions are $f(\alpha)=(1-\alpha)^2$, and the kinetic equations are $d\alpha/dt = 10^{19.24}(1-\alpha)^2 e^{-2.32\times10^4/T}$ and $d\alpha/dt = 10^{20.32}(1-\alpha)^2 e^{-2.43\times10^4/T}$. The thermal safety evaluation on the BTATz-CMDB propellants was obtained. With the substitution of 26% RDX by BTATz and with the help of the ballistic modifier in the CMDB propellant formulation, the burning rate can be improved by 89.0% at 8 MPa and 47.1% at 22 MPa, the pressure exponent can be reduced to 0.353 at 14–20 MPa.

1. Introduction

It is well known that the high-nitrogen energetic compounds derive most of their energy from the very large positive enthalpy of formation rather than from oxidation of the fuel-like carbon backbone. The materials are particularly suitable for consideration in high-performance propellant applications, because of their large positive enthalpy of formation, insensitivity to impact, friction and electrostatic discharge, and low-molecular-weight reaction products. 3,6-Bis (1H-1,2,3,4-tetrazol-5-yl-amino)-1,2,4,5-tetrazine (BTATz) is one of the high-nitrogen energetic compounds, with nitrogen content of 79.02%, density of 1.76 g cm^{-3}, enthalpy of formation of +883 kJ mol^{-1}, and moderate mechanical sensitivity [1–6]. As a substitute of hexogen (RDX) in the composite modified double base (CMDB) propellant formulation, BTATz can improve the burning rate and reduce the pressure exponent, it has a prospect using as a primary component in the high burning rate propellant for the booster rocket motor and the kinetic energy ammunition, and it also can be used in the minimum signature propellant for the smokeless ammunition [7–10]. In the work, the BTATz-CMDB propellants without and with the ballistic modifier were prepared, and their thermal behaviors, nonisothermal decomposition reaction kinetics, thermal safety and burning rates were investigated.

2. Experimental

2.1. Materials

BTATz used in the experiment was prepared by our research group [4]. ^{1}H NMR (DMSO-d_6, 500 MHz) (δ/ppm): 12.5 (s, 2H, NH). IR (KBr, υ/cm^{-1}): 3428, 3336, 1615, 1491, 1443, 1067. Ana1. calcd. for $C_4H_4N_{14}$: C 19.36, H 1.62, N 79.02; found C 19.51, H 1.78, N 78.90. Purity, 99.90% (measured by high-performance liquid chromatography); density, 1.72 g cm^{-3} (measured by pycnometer method, ammunition standard of China: GJB772A-97 401.1); impact sensitivity (drop height, H_{50}), 22.9 cm (measured by Bruceton staircase method, 5 kg drop weight, 50 mg sample mass, ammunition standard of China: GJB772A-97 601.2); friction sensitivity (probability of explosion, P), 64% (1.5 kg pendulum hammer fixed on 90° tilt angle, 3.92 MPa gauge pressure, 20 mg sample mass, ammunition standard of China: GJB772A-97 602.1); electrostatic spark sensitivity (E_{50}), 31.98 mJ [11].

The BTATz-CMDB propellant samples (nos. RB0601, RB0602) used in the experiment were composite modified double base

* Corresponding author. Tel.: +86 29 88291663; fax: +86 29 88220423.
E-mail addresses: yiren@nwu.edu.cn, npecc@21cn.com (F.-Q. Zhao).

0304-3894/$ – see front matter © 2010 Elsevier B.V. All rights reserved.
doi:10.1016/j.jhazmat.2010.05.029

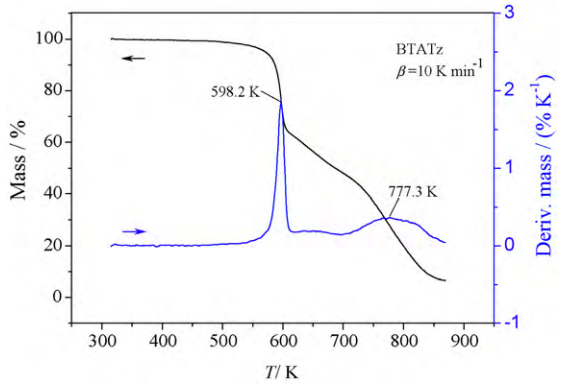

Fig. 1. TG-DTG curve for pure BTATz.

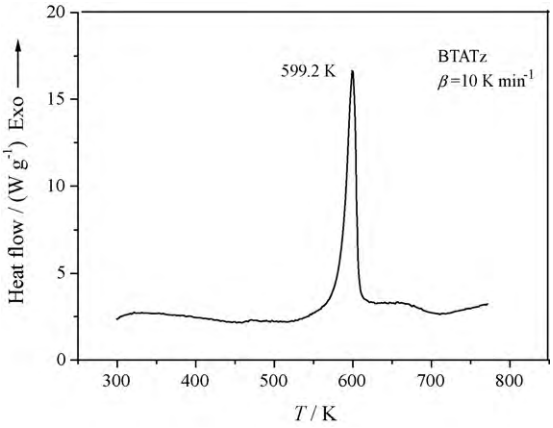

Fig. 2. DSC curve for pure BTATz.

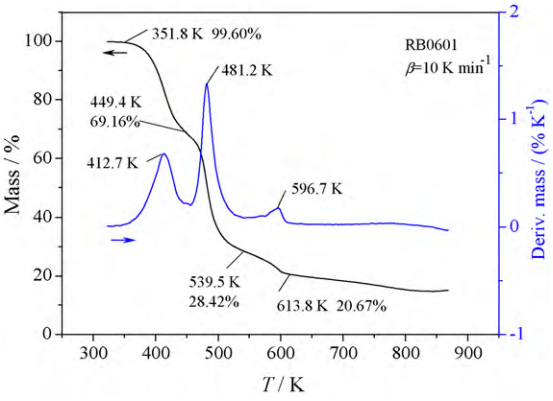

Fig. 3. TG-DTG curve for propellant RB0601.

propellant containing BTATz, composed of 38% (mass fraction) nitrocellulose (NC), 28% nitroglycerin (NG), 26% BTATz, 8% N-nitrodihydroxyethylamine-dinitrate (DINA) and other auxiliaries. The strand sample of the control propellant RB0601 composed of 500 g ingredients without ballistic modifier was prepared by a solventless CMDB propellant extrusion technique. The propellant RB0602 composed of 500 g ingredients with 17.5 g the mixture of lead phthalate, copper adipate and carbon black as a ballistic modifier was also prepared for the comparison with the control propellant RB0601.

2.2. Equipment and conditions

The TG-DTG and DSC curves under the condition of flowing nitrogen gas (purity, 99.999%; atmospheric pressure) were obtained by using a TA2950 thermal analyzer (TA Co., USA) and a 204HP differential scanning calorimeter (Netzsch Co., Germany). The conditions of TG-DTG were: sample mass, about 1 mg; N_2 flowing rate, 40 $cm^3\ min^{-1}$; heating rate (β), 10 $K\ min^{-1}$. The conditions of DSC analyses were: sample mass, about 1 mg; N_2 flowing rate, 50 $cm^3\ min^{-1}$; heating rate, 5, 10, 15, 20, 25, and 30 $K\ min^{-1}$; furnace pressures, 0.1 MPa; reference sample, α-Al_2O_3; type of crucible, aluminum pan with a pierced lid. The specific heat capacity (C_p, $J\ g^{-1}\ K^{-1}$) was determined with continuous C_p mode on a Micro-DSC III mircocalorimeter (Setaram Co., France), Heating rate, 0.15 $K\ min^{-1}$; sample mass, about 100 mg; atmosphere, N_2; reference sample, calcined α-Al_2O_3. And the specific heat capacity determined for the two propellant are: $C_p(J\ g^{-1}\ K^{-1})$ (RB0601) $= -3.90 + 3.10 \times 10^{-2}T - 4.40 \times 10^{-5}T^2$, $C_p(J\ g^{-1}\ K^{-1})$ (RB0602) $= -3.33 + 2.73 \times 10^{-2}T - 3.81 \times 10^{-5}T^2$. The burning rates of the samples were measured in a strand burner filled with nitrogen at different pressures, and the samples prepared were the $\Phi 5 \times 100$ mm cylinder strand coated with polyvinyl formal [12].

3. Results and discussion

3.1. Thermal behaviors

The TG-DTG curve and DSC curve for BTATz are shown in Figs. 1 and 2. The TG-DTG curves for the BTATz-CMDB propellants RB0601 and RB0602 are shown in Figs. 3 and 4, and the DSC curves at the heating rates of 5, 10, 15, 20, 25, and 30 $K\ min^{-1}$ are shown in Figs. 5 and 6.

From Figs. 3 and 4, one can find that there are three mass-loss stages (stages I–III) in TG curve, corresponding to the three peaks in DTG curve. For TG curve when $\beta = 10\ K\ min^{-1}$, stage I begins at about 350 K and stops at about 450 K, accompanying 24–30% mass-loss, which are close to the mass (28%) of NG, and it likely attributes to the volatilization and decomposition of NG, inducing the invisible peak in DSC curve of the temperature range of 350–550 K. Stage II begins followed by stage I and stops at about 530 K, with the summit peaks in DTG curves at about 480 K, accompanied by about 40% mass-loss, and it attributes to NG, DINA, NC and other auxiliary decomposition in the stage. Stage III stops at about 610 K, with the summit peak in DTG curve at about 590 K, accompanied by about 10% mass-loss, and it attributes to the decomposition of BTATz.

From Figs. 5 and 6, one can see that there are two exothermic peaks in DSC curve, the main exothermal decomposition peak corresponds to the stage II in TG curve, and the subordinate one corresponds to the stage III, caused by the decomposition of BTATz (see Figs. 1 and 2).

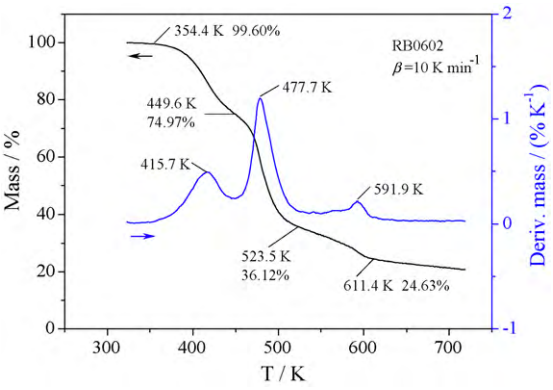

Fig. 4. TG-DTG curve for propellant RB0602.

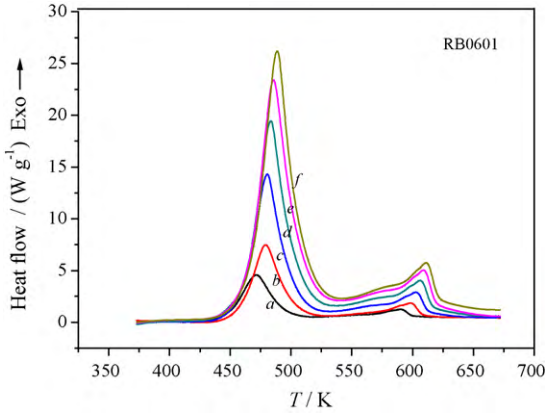

Fig. 5. DSC curves for propellant RB0601. Heating rate (K min^{-1}): (a) 5, (b) 10, (c) 15, (d) 20, (e) 25, and (f) 30.

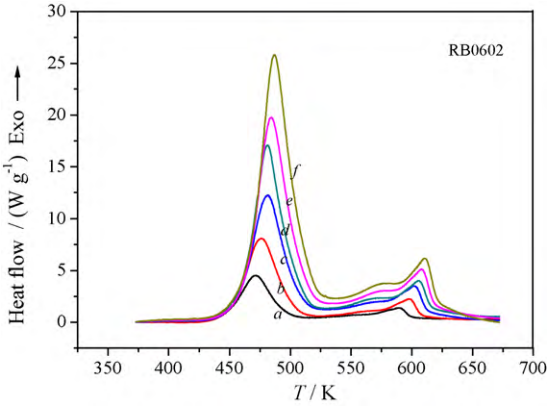

Fig. 6. DSC curves for propellant RB0602. Heating rate (K min^{-1}): (a) 5, (b) 10, (c) 15, (d) 20, (e) 25, and (f) 30.

The reason of the only one visible exothermic peak appears in the DSC curve during 350–550 K is that the two decomposition stages (stages I and II) occur in succession and the temperature ranges are near apart, the decomposition heats of the two processes overlap each other in DSC curve, inducing the only one exothermic peak to appear in the temperature range.

The basic data for the main exothermic decomposition processes of the propellants RB0601 and RB0602 are listed in Table 1.

Table 1
Basic data for the main exothermic decomposition processes of the propellants RB0601 and RB0602.

	β/(K min^{-1})	T_0/K	T_e/K	T_p/K	ΔH/(J g^{-1})
RB0601	5	415.5	449.7	471.4	1.55×10^3
	10	426.2	456.0	476.9	1.45×10^3
	15	430.1	458.0	480.5	1.57×10^3
	20	431.5	460.8	483.6	1.63×10^3
	25	432.9	463.3	485.6	1.59×10^3
	30	434.1	465.8	488.6	1.46×10^3
RB0602	5	417.1	450.8	471.5	1.60×10^3
	10	422.1	451.6	476.1	1.49×10^3
	15	424.1	456.2	481.4	1.45×10^3
	20	428.4	458.5	482.5	1.45×10^3
	25	428.9	461.7	485.3	1.39×10^3
	30	433.2	463.2	487.1	1.51×10^3

Note: T_0 is the initial temperature point at which DSC curve deviates from the base line; T_e is the onset temperature for the main exothermal decomposition reaction in DSC curve and T_p is the peak temperature; ΔH is the decomposition heat.

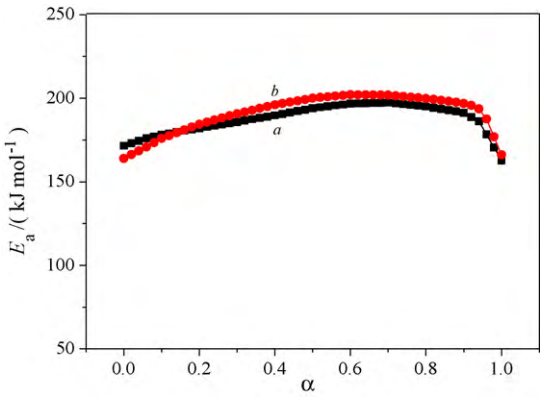

Fig. 7. E_a–α curves for the propellants RB0601 (a) and RB0602 (b).

3.2. Nonisothermal reaction kinetics

To explore the reaction mechanisms of the main exothermic decomposition processes of the propellants RB0601 and RB0602 and obtain the corresponding kinetic parameters [apparent activation energy (E_a/kJ mol^{-1}), pre-exponential constant (A/s^{-1})] and the most probable kinetic model functions, the DSC curves at the heating rates of 5, 10, 15, 20, 25, and 30 K min^{-1} were dealt with mathematic means, and the temperature data corresponding to the conversion degrees (α) were found. Five integral methods (General integral, MacCallum-Tanner, Šatava-Šesták, Agrawal, Flynn-Wall-Ozawa) and one differential method (Kissinger) were employed [11,13–15]. The values of E_a were obtained by Ozawa's method from the isoconversional DSC curves at the heating rates of 5, 10, 15, 20, 25, and 30 K min^{-1}, and the E_a–α relations are shown in Fig. 7. From Fig. 7, one can see that the activation energy changes slightly in the section of 0.08–0.98 (α) for curve (a), and 0.20–0.96 (α) for curve (b), and the sections were selected to calculate the nonisothermal reaction kinetics.

Forty-one types of kinetic model functions and the basic data for one propellant were put into the integral and differential equations for calculation, the values of E_a, lg$A$, linear correlation coefficient (r) and standard mean square deviation (Q) were calculated on computer with the linear least-squares method, and the most probable mechanism function is selected by the better values of r, and Q [13–15]. The results of satisfying the conditions at the same time are the final results as listed in Table 2, and the relevant function is the reaction mechanism function of the decomposition process.

From Table 2, one can find that the values of E_a and lg$A$ obtained from the nonisothermal DSC curves are in approximately good agreement with the values calculated by Kissinger's method and Ozawa's method, and the mechanism function number are determinated. The decomposition reaction mechanism functions of the propellants are listed in Table 3. Respectively substituting $f(\alpha)$ expression, and the values of E_a/(kJ mol^{-1}) and A/s^{-1} into Eq. (1), the corresponding kinetic equations [Eqs. (2) and (3)] of the decomposition reaction of the propellants are obtained and shown in Table 3.

$$\frac{d\alpha}{dt} = Af(\alpha)e^{-E/RT} \quad (1)$$

3.3. Thermal safety studies

3.3.1. Self-accelerating decomposition temperature (T_{SADT})

The values (T_{00}, T_{e0} and T_{p0}) of the initial temperature point at which DSC curve deviates from the base line (T_0), onset temperature (T_e) and peak temperature (T_p) corresponding to $\beta \to 0$ are obtained by Eq. (4), and the self-accelerating decomposition tem-

Table 2
Kinetic parameters for the main exothermic decomposition process of the propellants RB0601 and RB0602.

Method	β/(K min^{-1})	RB0601				RB0602			
		E_a/(kJ mol^{-1})	lg[A/(s^{-1})]	r	Q	E_a/(kJ mol^{-1})	lg[A/(s^{-1})]	r	Q
General integral	5	188.04	18.70	0.9983	0.3071	196.98	19.76	0.9997	0.0265
	10	190.57	18.99	0.9970	0.5366	207.43	20.98	0.9999	0.0079
	15	200.97	20.19	0.9965	0.6165	196.29	19.67	0.9991	0.0848
	20	196.59	19.69	0.9969	0.5398	203.44	20.56	0.9988	0.1148
	25	187.93	18.70	0.9950	0.8765	202.26	20.36	0.9987	0.1261
	30	193.75	19.32	0.9955	0.7847	206.42	20.79	0.9991	0.0885
Mac Callum-Tanner	5	188.75	18.74	0.9984	0.0568	197.74	19.81	0.9998	0.0048
	10	191.41	19.05	0.9973	0.0993	208.36	21.06	0.9999	0.0014
	15	201.93	20.27	0.9968	0.1144	197.25	19.74	0.9992	0.0155
	20	197.57	19.77	0.9972	0.1001	204.45	20.64	0.9989	0.0212
	25	188.92	18.77	0.9955	0.1627	203.33	20.45	0.9988	0.0233
	30	194.81	19.41	0.9960	0.1457	207.55	20.89	0.9992	0.0163
Šatava-Šesták	5	186.39	18.52	0.9984	0.0568	194.89	19.54	0.9998	0.0048
	10	188.91	18.82	0.9973	0.0993	204.91	20.73	0.9999	0.0014
	15	198.84	19.97	0.9968	0.1144	194.42	19.48	0.9992	0.0155
	20	194.73	19.50	0.9972	0.1001	201.22	20.34	0.9989	0.0212
	25	186.56	18.56	0.9955	0.1627	200.16	20.15	0.9988	0.0233
	30	192.12	19.16	0.9959	0.1457	204.14	20.57	0.9992	0.0163
Agrawal	5	188.04	18.70	0.9983	0.3071	196.98	19.76	0.9997	0.0265
	10	190.57	18.99	0.9970	0.5366	207.43	20.98	0.9999	0.0079
	15	200.97	20.19	0.9965	0.6165	196.29	19.67	0.9991	0.0848
	20	196.59	19.69	0.9969	0.5398	203.44	20.56	0.9988	0.1148
	25	187.93	18.70	0.9950	0.8765	202.26	20.36	0.9987	0.1261
	30	193.75	19.32	0.9955	0.7847	206.42	20.79	0.9991	0.0885
Mean		192.78	19.24			201.84	20.32		
Flynn-Wall-Ozawa		190.08 (E_{eO})		0.9934	0.0054	203.33 (E_{eO})		0.9522	0.0386
		192.45 (E_{pO})		0.9959	0.0034	203.98 (E_{pO})		0.9934	0.0054
Kissinger		194.40	19.51	0.9955	0.0182	206.53	20.88	0.9929	0.0287

Note: E with the subscript of eO, and pO is the apparent activation energy obtained from the onset temperature (T_e) and the peak temperature (T_p) by Ozawa's method.

Table 3
Mechanism functions, apparent activation energies and kinetic equations for the propellants RB0601 and RB0602.

	RB0601 (α = 0.08–0.98)	RB0602 (α = 0.20–0.96)
Mechanism function	$G(\alpha)=(1-\alpha)^{-1}-1$, $f(\alpha)=(1-\alpha)^2$, Chemical reaction	$G(\alpha)=(1-\alpha)^{-1}-1$, $f(\alpha)=(1-\alpha)^2$, Chemical reaction
Mech funct.no.	37	37
E_a/(kJ mol^{-1})	192.78	201.84
Kinetic equation	$\frac{d\alpha}{dt}=10^{19.24}(1-\alpha)^2e^{-2.32\times10^4/T}$ (2)	$\frac{d\alpha}{dt}=10^{20.32}(1-\alpha)^2e^{-2.43\times10^4/T}$ (3)

perature (T_{SADT}) is obtained by Eq. (5) [13–15]. The values of the propellants are listed in Table 4.

$$T_{0(\text{or e or p})} = T_{00\,(\text{or e0 or p0})} + b\beta + c\beta^2 + d\beta^3 + e\beta^4 \quad (4)$$

where b, c, d and e are coefficients.

$$T_{SADT} = T_{e0} \quad (5)$$

Table 4
The derivative parameters for RB0601 and RB0602.

	RB0601	RB0602
T_{00}/K	391.2	413.3
T_{SADT}/K	434.1	456.6
T_{p0}/K	464.5	467.1
T_{TIT}/K	442.7	465.5
T_b/K	474.2	476.4
t_{TIAD}/s	51.5	3.4
$\Delta S^{\neq}$/(J mol^{-1} K^{-1})	116.58	142.76
$\Delta H^{\neq}$/(kJ mol^{-1})	190.54	202.62
$\Delta G^{\neq}$/(kJ mol^{-1})	136.38	135.93
$T_{cr,hot\text{-}spot}$/K	642.6	633.9

3.3.2. Thermal ignition temperature (T_{TIT}) and critical temperatures of thermal explosion (T_b)

The thermal ignition temperature (T_{be0} or T_{TIT}) is obtained by substituting E_{eO} and T_{e0} into Zhang et al. equation [Eq. (6)] [16], and the critical temperatures of thermal explosion (T_{bp0} or T_b) is obtained by substituting E_{pO} and T_{p0} into the equation. The values are listed in Table 4. The high values of T_b for the BTATz-CMDB propellants show that the transition from thermal decomposition to thermal explosion is not easy to take place.

$$T_{be0(\text{or bp0})} = \frac{E_O - \sqrt{E_O^2 - 4E_O R T_{e0\,(\text{or p0})}}}{2R} \quad (6)$$

3.3.3. Adiabatic time-to-explosion (t_{TIAD})

The adiabatic time-to-explosion (t_{TIAD}) of energetic materials (EMs) is the time of decomposition transiting to explosion under the adiabatic conditions and is an important parameter for assessing their thermal stability and the safety.

$$t_{Tlad} = \int_0^t dt = \frac{1}{Q_d A}\int_{T_{e0}}^{T_{bp0}} \frac{C_p \exp(E/RT)}{f(\alpha)} dT \quad (7)$$

$$\alpha = \int_{T_{e0}}^{T_{bp0}} \frac{C_p}{Q_d} dT \quad (8)$$

Table 5
Explosive parameters and comparison of experimental and predicted 50% drop height of impact sensitivity (H_{50}).

No.	Sample	λ/(10^{-4} J cm^{-1} s^{-1} K^{-1})(1)	ρ/(g cm^{-3})	$lg[A/(s^{-1})]$(2)	Q_d/(J g^{-1})(3)	$_E$/(J mol^{-1})(2)	H_{50}/cm (Exp.)(1)	H_{50}/cm (Predicted)	n	D_2	D_3
1	HMX	34.43	1.79	33.80	2764	373700	32	33.4	0.564623	33.8765	−0.347174
2	RDX	10.58	1.66	12.50	2810	140000	26	20.1			
3	TNT	21.30	1.57	11.10	1506	155017	59	56.4			
4	PETN	25.10	1.68	10.40	3263	112300	16	15.60			
5	BTF	20.92	1.81	22.81	2949	255000	28	30.0			
6	HNS	8.53	1.65	22.63	1389	289000	54	50.1			
7	Tetryl	18.74	1.67	16.90	1904	172500	17(4)	17.6			
8	NG	12.55	1.60	16.09	2092	150122	7(4)	9.4			
9	RB0601	20.0	1.655	19.51	1540	194400		17.4			
10	RB0602	30.0	1.660	20.88	1480	206530		18.1			

Note: (1) Cited from Ref. [21]; (2) cited from Ref. [22]; (3) cited from Ref. [23]; (4) cited from Ref. [24]. T_{room} = 350.15 K.

Table 6
The calculated values of $T_{S(T)max}$, S_d, T_{acr} and P_{TE} for propellants RB0601 and RB0602.

	Infinite plate				Infinite cylinder				Sphere sample			
	$T_{S(T)max}$/K	S_d/%	T_{acr}/K	P_{TE}/%	$T_{S(T)max}$/K	S_d/%	T_{acr}/K	P_{TE}/%	$T_{S(T)max}$/K	S_d/%	T_{acr}/K	P_{TE}/%
RB0601	355.5	41.46	350.7	58.54	360.0	51.82	355.2	48.18	362.8	57.24	358.0	42.76
RB0602	362.7	56.42	357.9	43.58	367.1	62.79	362.3	37.21	369.9	65.63	365.1	34.37

where C_p is the specific heat capacity measured by mircocalorimeter in J g^{-1} K^{-1}, Q_d is the average value of the decomposition heats (H) at the six heating rates in J g^{-1}, A is the pre-exponential constant in s^{-1} and $A = A_K$, E is the apparent activation energy in J mol^{-1} and $E = E_K$, R is the gas constant in J mol^{-1} K^{-1}, $f(\alpha)$ is the decomposition reaction mechanism function.

Substituting the corresponding data into Smith equation [Eqs. (7) and (8)] [17,18], the values of t_{TIAD} for the propellants are acquired and listed in Table 4.

From Table 4, one can find that (1) $T_{SADT,\ RB0601} < T_{SADT,\ RB0602}$, $T_{TIT,RB0601} < T_{TIT,\ RB0602}$, and $T_{b,\ RB0601} < T_{b,\ RB0602}$, which means that the propellant RB0602 has a higher resistance to heat and thermal safety than RB0601 under the same experimental conditions; (2) $t_{TIAD,\ RB0601} > t_{TIAD,\ RB0602}$, which means that the transition from adiabatic decomposition to explosion for propellant RB0602 is easier than RB0601.

3.3.4. Thermodynamic parameters of activation reaction

The entropy of activation ($\Delta S^{\neq}$), enthalpy of activation ($\Delta H^{\neq}$), and free energy of activation ($\Delta G^{\neq}$) of the main exothermic decomposition reaction of the propellants, corresponding to $T = T_{p0}$, $E = E_K$, and $A = A_K$, are obtained by Eqs. (9)–(11) [13,14], and listed in Table 4. The positive values of $\Delta G^{\neq}$, indicate that the exothermic decomposition reaction of the propellants must proceed under the heating condition.

$$A\exp(-E/RT) = (k_B T/h)\exp(-\Delta G^{\neq}/RT) \tag{9}$$

$$\Delta H^{\neq} = E - RT \tag{10}$$

$$\Delta G^{\neq} = \Delta H^{\neq} - T\Delta S^{\neq} \tag{11}$$

3.3.5. Critical temperature of hot-spot initiation ($T_{cr,hot\text{-}spot}$)

In order to obtain the critical temperature of hot-spot initiation ($T_{cr,hot\text{-}spot}$) of the propellants, assuming that $T_{cr,hot\text{-}spot}$ is a function of the size and duration of the hot-spot and of the physical and chemical properties, the equation for calculating the value of $T_{cr,hot\text{-}spot}$ can be adopted as Bruckman–Guillet first-order decomposition reaction estimation equation [Eq. (12)] [19,20].

$$\left(\frac{4}{3}\pi a^3\right)\rho Q_d\{1-\exp[-(t-t_0)Ae^{-E/RT_{cr,hot\text{-}spot}}]\} = \int_a^{\infty} 4\pi r^2 \rho C_p \times \left[\frac{a\theta_0}{r}\mathrm{erfc}\left[\frac{r-a}{2\sqrt{Bt}}\right]\right]\mathrm{d}r = \int_a^{\infty} 4\pi r^2 \rho C_p \times \left[\frac{a(T_{cr,hot\text{-}spot}-T_{room})}{r}\mathrm{erfc}\left[\frac{(r-a)}{2\sqrt{(\lambda/\rho C_p)t}}\right]\right]\mathrm{d}r \tag{12}$$

where a is the radius of the hot-spot in 10^{-3} cm, ρ is the density in g cm^{-3}, Q_d is the heat of reaction in J g^{-1}, $t - t_0$ is the time interval in 10^{-4} s, A is the pre-exponential constant in s^{-1} and $A = A_K$, E is the apparent activation energy in J mol^{-1} and $E = E_K$, R is the gas constant in J mol^{-1} K^{-1}, $T_{cr,\ hot\text{-}spot}$ is the critical temperature of hot-spot initiation in K, C_p is the specific heat in J g^{-1} K^{-1}, T_{room} is the ambient temperature in 293.15 K, λ is the thermal conductivity in J cm^{-1} s^{-1} K^{-1}.

For the propellant RB0601: the thermal conductivity $\lambda = 20 \times 10^{-4}$ J cm^{-1} s^{-1} K^{-1}, $\rho = 1.655$ g cm^{-3}; for the propellant RB0602: $\lambda = 30 \times 10^{-4}$ J cm^{-1} s^{-1} K^{-1}, $\rho = 1.660$ g cm^{-3}.

Substituting the corresponding data into Eq. (12), and the values of $T_{cr,hot\text{-}spot}$ are acquired and listed in Table 4.

3.3.6. Characteristic drop height of impact sensitivity (H_{50})

To obtain the characteristic drop height of impact sensitivity (H_{50}) of the propellants, substituting the values of the thermal conductivity (λ), the density (ρ), A, Q_d and E of eight explosives with known 50% drop height listed in Table 5 into Eq. (13) [21–24], the corresponding values of the parameter n of 0.564623, D_2 of 33.8765, and D_3 of −0.347174 are obtained. By substituting the values of λ, ρ, A, Q_d and E of the propellants listed in Table 5 and the values of n, D_2 and D_3 into Eq. (13), the corresponding the value of H_{50} of 17.4 cm for RB0601 and 18.1 cm for RB0602 are obtained, showing that they have impact sensitivity level approaching that of RDX.

$$\frac{1}{2}n\lg H_{50} + \lg\sqrt{\frac{\lambda}{A\rho Q_d}} + D_3 + \frac{0.02612E}{T_1 + D_2 H_{50}^n} = 0 \tag{13}$$

3.3.7. Critical thermal explosion ambient temperature (T_{acr}), thermal sensitivity probability density function [$S(T)$], safety degree (S_d) and thermal explosion probability (P_{TE})

In order to explore the heat-resistance ability of the propellants, the values of the critical thermal explosion ambient temperature (T_{acr}), the thermal sensitivity probability density function [$S(T)$], the safety degree (S_d) and the thermal explosion probability (P_{TE}) are calculated by Frank–Kamenetskii formula [Eq. (14)] [25], Wang-Du formula [Eqs. (15)–(19)] and Eq. (20) [26–28]. In these formulas, A is the pre-exponential constant in s^{-1} and $A = A_K$, E is the apparent activation energy in J mol^{-1} and $E = E_K$, R is the gas constant in J K^{-1} mol^{-1}, λ is the thermal conductivity in W m^{-1}K^{-1}, δ is the Frank–Kamenetskii (FK) parameter, δ_{cr} is the criticality of thermal explosion of exothermic system, r is characteristic measurement of reactant in 1.0 m, Q_d is decomposition heat in J g^{-1}, ρ is density in g cm^{-3}, μ_T is the average value of temperature in K, σ_δ is the standard deviation of FK parameter, σ_T is the standard deviation of ambient temperature in 10 K, T is the surrounding temperature in 350.15 K.

The maximum value of $S(T)$ vs T relation curve ($T_{S(T)max}$), S_d, T_{acr} and P_{TE} of the propellant are obtained and shown in Table 6.

$$T_{acr} = \frac{-E}{2R\,\mathrm{Lambert}\,W_{-1}\left(-(1/2)\sqrt{(\lambda E\delta_{cr}/r^2 Q\rho AR)}\right)} \tag{14}$$

$$W = \frac{r^2 Q_d E_K \rho A_K}{\lambda R} \tag{15}$$

$$\mu_T = \frac{-E_K}{2R\,\mathrm{Lambert}W_{-1}\left(-(1/2)\sqrt{(\lambda E_K\delta_{cr}/r^2 Q_d\rho A_K R)}\right)} \tag{16}$$

$$\sigma_\delta = W\left(\frac{E_K - 2R\mu_T}{R\mu_T^4}\right)\exp\left(-\frac{E_K}{R\mu_T}\right)\sigma_T \tag{17}$$

$$S(T) = \frac{W(E_K - 2RT)}{\sqrt{2\pi}\sigma_\delta RT^4}\exp\left\{\frac{-[W(\exp(-(E_K/RT))/T^2) - \delta_{cr}]^2}{2\sigma_\delta^2 - (E_K/RT)}\right\} \tag{18}$$

$$S_d = \int_0^{+\infty}\int_0^{+\infty}\frac{W(E_K - 2RT)}{2\pi\sigma_\delta\sigma_T RT^4}\exp \times\left\{-\frac{[W((\exp(-E_K/RT))/T^2) - \mu_\delta]^2}{2\sigma_\delta^2 - (E_K/RT) - (Y - T + \mu_T)^2/(2\sigma_T^2)}\right\}\mathrm{d}T\mathrm{d}y \tag{19}$$

$$P_{TE} = 1 - S_d \tag{20}$$

The calculated values of $T_{S(T)max}$, S_d, T_{acr} and P_{TE} for the propellants RB0601 and RB0602 show that (1) $T_{S(T)max,RB0601} < T_{S(T)max,RB0602}$, $S_{d,RB0601} < S_{d,RB0602}$, and $T_{acr,RB0601} < T_{acr,RB0602}$, which means that the propellant RB0602 has a higher resistance to heat and thermal safety than RB0601 under the same experimental conditions; (2) $T_{S(T)max,\ infinite\ plate} < T_{S(T)max,\ infinite\ cylinder} < T_{S(T)max\ sphere\ sample}$, $S_{d,Infinite\ plate} < S_{d,\ infinite\ cylinder} < S_{d,\ sphere\ sample}$, and $T_{acr,\ infinite\ plate} < T_{acr,\ infinite\ cylinder} < T_{acr,\ sphere\ sample}$, which means that the sphere charge is more safe than another with the

Table 7
Burning rates (mm s^{-1}) of the RDX-CMDB propellant (System I), RB0601 (System II) and RB0602 (System III).

System	P/MPa										
	2	4	6	8	10	12	14	16	18	20	22
I	3.09	5.34	7.42	9.85	11.88	14.04	15.75	17.54	19.23	20.92	21.86
II	4.66	8.41	11.52	14.51	17.36	19.47	21.88	24.04	26.53	28.13	30.30
III	6.24	9.88	14.01	18.62	21.95	25.00	27.10	28.49	29.59	30.77	32.15

same characteristic measurement under the same experimental conditions.

3.4. Burning rate measurement

For the sake of the possible application of BTATz in CMDB propellant, the burning rates [u/(mm s^{-1})] of the RDX-CMDB propellant (system I, mass fraction, NC/NG/RDX/auxiliary = 38/28/26/8) and the two BTATz-CMDB propellants (RB0601, system II; RB0602, system III) were measured under different pressures (P/MPa). The results are listed in Table 7. As one can see, with the substitution of 26% RDX by BTATz in CMDB propellant formulation, the burning rate can be improved by 47.3% at 8 MPa and 38.6% at 22 MPa, and even higher with the help of the ballistic modifier, it can be improved by 89.0% at 8 MPa and 47.1% at 22 MPa.

In order to evaluate the effects of the ballistic modifier on the burning rates of the BTATz-CMDB propellant, the pressure exponent (n) of the burning rate (u) was calculated, and the mean value of the catalysis efficiency ($\overline{Z}$) was compared before and after ballistic modifier was added into the propellant formulation. The values of n, and $\overline{Z}$ were obtained by Eqs. (21) and (22) [29,30].

$$ui = aP_i^n, \quad i = 1 - 11, \tag{21}$$

$$\overline{Z} = \sum_{i=1}^{k} \frac{(u_{\mathrm{III},\,i}/u_{\mathrm{II},i})}{k} \tag{22}$$

where a is the factor, mm s^{-1} MPa^{-1}.

For system II: at 8–22 MPa, $u = 3.25P^{0.723}$, $r = 0.999$, $\overline{Z} = 1$; at 10–22 MPa, $u = 3.33P^{0.714}$, $r = 0.999$, $\overline{Z} = 1$; at 14–20 MPa, $u = 3.28P^{0.719}$, $r = 0.995$, $\overline{Z} = 1$.

For system III: at 8–22 MPa, $u = 6.58P^{0.522}$, $r = 0.973$, $\overline{Z} = 1$; at 10–22 MPa, $u = 13.57P^{0.459}$, $r = 0.978$, $\overline{Z} = 1.17$; at 14–20 MPa, $u = 10.69P^{0.353}$, $r = 0.999$, $\overline{Z} = 1.16$.

As one can see, as a ballistic modifier, the mixture of lead phthalate, copper adipate and carbon black can be effective to accelerate the burning rate and reduce the pressure exponent of the BTATz-CMDB propellant.

4. Conclusions

The BTATz-CMDB propellants (nos. RB0601 and RB0602) without and with the ballistic modifier were prepared. There are three mass-loss stages in TG curve for the BTATz-CMDB propellant, and they are likely attributes to the volatilization of NG, the decomposition of NG, NC, DINA and other auxiliary, and the decomposition of BTATz. The first two mass-loss stages occur in succession and the temperature ranges are near apart, the decomposition peaks of the two stages overlap each other, inducing only one visible exothermic peak appear in DSC curve during 350–550 K. The reaction mechanisms of the main exothermal decomposition processes of RB0601 and RB0602 are classified as chemical reaction, and $f(\alpha) = (1-\alpha)^2$. The kinetic equations are: $\mathrm{d}\alpha/\mathrm{d}t = 10^{19.24}(1-\alpha)^2 e^{-2.32\times10^4/T}$ and $\mathrm{d}\alpha/\mathrm{d}t = 10^{20.32}(1-\alpha)^2 e^{-2.43\times10^4/T}$. The results of evaluating the thermal safety of the propellants were obtained as: the propellant RB0602 has a higher resistance to heat and thermal safety than RB0601; the transition from adiabatic decomposition to explosion for propellant RB0602 is easier than RB0601; the sphere charge is safer than another with the same characteristic measurement. With the substitution of 26% RDX by BTATz and with the help of the ballistic modifier in the CMDB propellant formulation, the burning rate can be improved by 89.0% at 8 MPa and 47.1% at 22 MPa, the pressure exponent can be reduced to 0.353 at 14–20 MPa.

Acknowledgements

This work was supported by the National Natural Science Foundation of China (no. 20573098) and the Foundation of National Key Laboratory of Science and Technology on Combustion (no. 9140C3503020804).

References

[1] M.A. Hickey, D.E. Chavez, D. Naud, Preparation of 3,3′-azobis (6-amino-1,2,4,5-tetrazine), US Patent 6342589, 2002.
[2] M.A. Hickey, D.E. Chavez, D. Naud, 3,6-Bis(1H-1,2,3,4-tetrazol-5-yl-amino)-1,2,4,5-tetrazine or salt thereof, US Patent 6657059, 2003.
[3] S.T. Yue, S.Q. Yang, Synthesis and properties of 3,6-bis (1H-1,2,3,4-tetrazol-5-yl-amino)-1,2,4,5-tetrazine, Chin. J. Energy Mater. 12 (3) (2004) 155–157.
[4] B.Z. Wang, W.P. Lai, Q. Liu, P. Lian, Y.Q. Xue, Synthesis, characterization and quantum chemistry study on 3,6-bis (1 H-1,2,3,4-tetrazol-5-yl-amino)-1,2,4,5-tetrazine, Chin. J. Org. Chem. 28 (3) (2008) 422–427.
[5] A. Saikia, R. Sivabalan, B.G. Polke, G.M. Gore, A. Singh, A. Subhananda Rao, A.K. Sikder, Synthesis and characterization of 3,6-bis(1H-1,2,3,4-tetrazol-5-ylamino)-1,2,4,5-tetrazine (BTATz): novel high- nitrogen content insensitive high energy material, J. Hazard. Mater. 170 (2009) 306–313.
[6] X.G. Zhang, H. Zhu, S.Q. Yang, W. Zhang, F.Q. Zhao, Z.R. Liu, Q. Pan, Study on thermal decomposition kinetics and mechanism of nitrogen-rich compound BTATz, Chin. J. Prop. Technol. 28 (3) (2007) 322–326.
[7] S.F. Son, H.L. Berghout, C.A. Bolme, D.E. Chavez, D. Naud, M.A. Hiskey, Burn rate measurements of HMX, TATB, DHT, DAAF, and BTATz, Proc. Combust. Inst. 28 (2000) 919–924.
[8] M.A. Hickey, D.E. Chavez, D. Naud, Low-smoke pyrotechnic compositions, US Patent 6312537, 2001.
[9] S.W. Li, F.Q. Zhao, C. Yuan, Y. Luo, Y. Gao, Tendency of research and development for overseas solid propellants, Chin. J. Solid Rocket Tech. 25 (2) (2002) 36–42.
[10] M.A. Hickey, D.E. Chavez, D. Naud, Propellant containing 3,6-bis(1H-1,2,3,4-tetrazol-5-yl-amino)-1,2,4,5 -tetrazine or salts thereof, US Patent 6458227, 2002.
[11] J.H. Yi, F.Q. Zhao, H.X. Gao, S.Y. Xu, M.C. Wang, R.Z. Hu, Preparation, characterization, nonisothermal reaction kinetics, thermodynamic properties, and safety performances of high nitrogen compound: hydrazine 3-nitro-1,2,4-triazol-5-one complex, J. Hazard. Mater. 153 (2008) 261–268.
[12] F.Q. Zhao, H.X. Gao, Y. Luo, R.Z. Hu, C. Pei, S.L. Gao, X.W. Yang, Q.Z. Shi, Constant-volume combustion energy of the lead salts of 2HDNPPb and 4HDNPPb and their effect on combustion characteristics of RDX-CMDB propellant, J. Therm. Anal. Cal. 85 (3) (2006) 791–794.
[13] R.Z. Hu, S.L. Gao, F.Q. Zhao, Q.Z. Shi, T.L. Zhang, J.J. Zhang, Thermal Analysis Kinetics, second ed., Science Press, Beijing, 2008.
[14] F.Q. Zhao, R.Z. Hu, H.X. Gao, H.X. Ma, Thermochemical properties, nonisothermal decomposition reaction kinetics and quantum chemical investigation of 2,6-diamino-3,5-dinitropyrazine-1-oxide (LLM-105), in: O.E. Bronna (Ed.), New Developments in Hazardous Materials Research, Nova Science Publishers Inc., New York, 2006 (chapter 4).
[15] H.X. Ma, J.R. Song, F.Q. Zhao, R.Z. Hu, H.M. Xiao, Nonisothermal reaction kinetics and computational studies on the properties of 2,4,6,8-tetranitro-2,4,6,8-tetraazabicyclo [3,3,1] onan-3,7-dione (TNPDU), J. Phys. Chem. A 111 (2007) 8642–8649.
[16] T.L. Zhang, R.Z. Hu, Y. Xie, F.P. Li, The estimation of the critical temperature of thermal explosion for energetic materials using non-isothermal DSC, Thermochim. Acta 244 (1994) 171–176.
[17] L.C. Smith, An approximate solution of the adiabatic explosion problem, Thermochim. Acta 13 (1) (1975) 1–6.
[18] R.Z. Hu, H. Zhang, Z.M. Xia, P.J. Guo, S.L. Gao, Q.Z. Shi, G.E. Lu, J.Y. Jiang, Estimation formulae of the critical rate of temperature rise for thermal explosion

of exothermic decomposition reaction system of energetic materials, Chin. J. Energy Mater. 11 (3) (2003), 130-133, 137.
[19] H.J. Bruckman, J.E. Guillet, Theoretical calculations of hot-spot initiation in explosives, Can. J. Chem. 41 (1968) 3221–3228.
[20] R.Z. Hu, H.X. Gao, F.Q. Zhao, H. Zhang, M. Gou, H.A. Zhao, X.J. Wang, H.X. Ma, Estimation of critical temperatures of hot-spot initiation in energetic materials, Chin. J. Energy Mater. 17 (2) (2009) 127–130.
[21] H.S. Dong, F.F. Zhou, Performances of High Explosive and its Related Materials, Science Press, Beijing, 1989.
[22] H.S. Dong, R.Z. Hu, P. Yao, X.X. Zhang, Thermograms of Energetic Materials, National Defence Industry Press, Beijing, 2001.
[23] R.Z. Hu, F.Q. Zhao, H.X. Gao, H. Zhang, H.A. Zhao, X.J. Wang, X.L. Zhang, Y. Feng, H.X. Ma, The estimation of characteristic drop heights of impact sensitivity for polymer bonded explosives JH-94 and JO-96, Chin. J. Energy Mater. 17 (3) (2009) 251–254.
[24] M.H. Friedman, A correlation of impact sensitivities by means of the hot spot model, in: 9th (international) Symposium on Combustion, Academic Press Inc, New York, 1963, pp. 294–302.
[25] D.A. Frank-Kamenetskii, Diffusion and Heat Exchange in Chemical Kinetics, Princeton University Press, Princeton, 1955.
[26] P. Wang, Z.M. Du, Probability distribution of thermal sensitivity of energetic materials, Chin. J. Energy Mater. 15 (6) (2007) 633–636.
[27] P. Wang, Study on thermal safety and ignition reliability of exothermic system, Ph.D. Dissertation, Beijing Institute of Technology, 2008.
[28] R.Z. Hu, H.X. Gao, F.Q. Zhao, Thermal safety of plastic bonded explosives JH-94 and JO-96, Chin. J. Explos. Propell. 31 (6) (2008) 28–31.
[29] P. Chen, F.Q. Zhao, Y. Luo, R.Z. Hu, S.L. Gao, Y.M. Zheng, M.Z. Deng, Y. Gao, Thermal decomposition behavior and non-isothermal decomposition reaction of copper(II) salt of 4-hydroxy-3,5-dinitropyridine oxide and its application in solid rocket propellant, Chin. J. Chem. 22 (2004) 1056–1063.
[30] J.H. Yi, F.Q. Zhao, W.L. Hong, S.Y. Xu, R.Z. Hu, Z.Q. Chen, L.Y. Zhang, Effects of Bi-NTO complex on thermal behaviors, nonisothermal reaction kinetics and burning rates of NG/TEGDN/NC propellant, J. Hazard. Mater. 176 (2010) 257–261.